Argonne NATIONAL LABORATORY

ANL-GenIV-55

Topical Report:

CFD Analysis for the Applicability of the Natural Convection Shutdown Heat Removal Test Facility (NSTF) for the Simulation of the VHTR RCCS

Nuclear Engineering Division

About Argonne National Laboratory

Argonne is a U.S. Department of Energy laboratory managed by UChicago Argonne, LLC under contract DE-AC02-06CH11357. The Laboratory's main facility is outside Chicago, at 9700 South Cass Avenue, Argonne, Illinois 60439. For information about Argonne, see www.anl.gov.

Availability of This Report

This report is available, at no cost, at http://www.osti.gov/bridge. It is also available on paper to the U.S. Department of Energy and its contractors, for a processing fee, from:

U.S. Department of Energy
Office of Scientific and Technical Information
P.O. Box 62
Oak Ridge, TN 37831-0062
phone (865) 576-8401
fax (865) 576-5728
reports@adonis.osti.gov

ANL-GenIV-55

Topical Report:

CFD Analysis for the Applicability of the Natural Convection Shutdown Heat Removal Test Facility (NSTF) for the Simulation of the VHTR RCCS

by
C. P. Tzanos
Nuclear Engineering Division, Argonne National Laboratory

September 2005

work sponsored by

U. S. Department of Energy,
Office of Nuclear Energy, Science and Technology

UChicago ▶ Argonne LLC

Office of Science
U.S. DEPARTMENT OF ENERGY

A U.S. Department of Energy laboratory managed by UChicago Argonne, LLC

Table of Contents

1.0 Introduction 6

2.0 Model Description 6

2.1. CFD Model of the RCCS in the Plant Geometry 7

2.2. CFD Model of the RCCS at NSTF 7

2.3. Pressure Drop Model (including stack) 9

3.0 Plant RCCS Performance 11

3.1. Uniform Reactor Vessel Temperature of 480°C (GT-MHR Steady State) 12

3.2. RCCS Performance at VHTR Conditions 14

4.0 NSTF Performance 16

4.1. Uniform Heated Wall Temperature of 480 °C 16

4.2. Uniform Heated Wall Temperature of 677 °C 17

5.0 Conclusions 18

37. Reactor vessel temperature distribution (VHTR1000) 44
38. Air temperature distribution along the RCCS tube (VHTR1000) 44
39. Tube and air temperature distribution at 5.3 m (VHTR1000) 45
40. Heat transfer coefficients (VHTR1000) 46
41. Nusselt number vs. tube height 46
42. Grashof and Rayleigh numbers vs. tube height (VHTR1000) 47
43. Buoyancy number vs. tube height 47
44. NSTF tube temperature distribution at 6.7 m (heated wall temperature of 480 °C) 48
45. NSTF heat transfer coefficient (heated wall temperature of 480 °C) 48
46. Variation of heat transfer coefficient around the tube walls (NSTF heated wall temperature of 480 °C 49
47. Variation of heat flux around the tube walls (NSTF heated wall temperature of 480 °C) 49
48. Heat transfer coefficient for a constant air thermal conductivity (NSTF heated wall temperature of 480 °C) 50
49. Reynolds number versus tube height 50
50. Grashof and Rayleigh numbers versus tube height (NSTF heated wall temperature of 480 °C) 51
51. Buoyancy number versus tube height (NSTF heated wall temperature of 480 °C) 51
52. Nusselt number versus NSTF tube height (NSTF heated wall temperature of 480 °C) 52
53. Grashof and Rayleigh numbers; front wall of NSTF tube (based on hydraulic diameter and heated wall temperature of 480 °C) 53
54. Buoyancy number; front wall of NSTF (based on hydraulic diameter and heated wall temperature of 480 °C) 53
55. NSTF tube temperature distribution at 6.7 m (heated wall temperature of 677 °C) 54
56. Heat transfer coefficient for an NSTF heated wall temperature of 677 °C 55
57. Grashof and Rayleigh numbers for an NSTF heated wall temperature of 677 °C 55
58. Buoyancy number (NSTF heated wall temperature of 677 °C) 56
59. Grashof and Rayleigh numbers; front wall of NSTF tube (based on hydraulic diameter and heated wall temperature of 677 °C) 56
60. Buoyancy number; front wall of NSTF tube (based on hydraulic diameter and heated wall temperature of 677 °C) 57
61. Nusselt number along the axis of the NSTF tube walls (heated wall temperature of 677 °C) 57
62. Nusselt number along the axis of the RCCS tube walls (reactor vessel temperature of 560 °C) 58

1.0. INTRODUCTION

The Very High Temperature gas cooled reactor (VHTR) is one of the GEN IV reactor concepts that have been proposed for thermochemical hydrogen production and other process-heat applications like coal gasification. The United States Department of Energy has selected the VHTR for further research and development, aiming to demonstrate emissions-free electricity and hydrogen production at a future time.

One of the major safety advantages of the VHTR is the potential for passive decay heat removal by natural circulation of air in a Reactor Cavity Cooling System (RCCS). The air-side of the RCCS is very similar to the Reactor Vessel Auxiliary Cooling System (RVACS) that has been proposed for the PRISM reactor design. The design and safety analysis of the RVACS have been based on extensive analytical and experimental work performed at ANL. The Natural Convection Shutdown Heat Removal Test Facility (NSTF) at ANL that simulates at full scale the air-side of the RVACS was built to provide experimental support for the design and analysis of the PRISM RVACS system. The objective of this work is to demonstrate that the NSTF facility can be used to generate RCCS experimental data: to validate CFD and systems codes for the analysis of the RCCS; and to support the design and safety analysis of the RCCS.

At this time no reference design is available for the NGNP. The General Atomics (GA) gas turbine – modular helium reactor (GT-MHR) has been used in many analyses as a starting reference design [1]. In the GT-MHR the reactor outlet temperature is 850 °C, while the target outlet reactor temperature in VHTR is 1000 °C. VHTR scoping studies with a reactor outlet temperature of 1000 °C have been performed at GA and INEL. Although the reactor outlet temperature in the VHTR is significantly higher than in the GT-MHR, the peak temperature in the reactor vessel (which is the heat source for the RCCS) is not drastically different. In this work, analyses have been performed using reactor vessel temperatures from the GT-MHR design, and the VHTR scoping studies.

To demonstrate the applicability of the NSTF facility for full scale simulation of the RCCS the following approach was used. CFD analyses were performed of the RCCS and of its simulation at NSTF to demonstrate that: all significant fluid flow and heat transfer phenomena in the RCCS can be simulated at NSTF; and RCCS simulations at NSTF can cover the whole range of variation of the parameters describing these important phenomena in the RCCS.

In CFD analyses, the simulation of turbulence is one of the most significant challenges. Direct Numerical Simulation (DNS) and Large Eddy Simulation (LES) of turbulence in large scale systems require excessive computational resources. The use of the Low-Re number k-ε model, which resolves the boundary layer, is computationally expensive in studies where many simulations have to be performed. In Ref. 2 it was shown that in the RCCS, heat transfer coefficient predictions of the high-Re number k-ε model are closer to those of the low-Re number model than those of heat transfer correlations. In this work, the standard high-Re number k-ε was used to simulate turbulence, and all analyses were performed with the CFD code STAR-CD.

2.0. MODEL DESCRIPTION

For the purpose of this project two STAR-CD models were constructed. One model simulated the RCCS and its environs within the plant. The second model simulated the RCCS in the environs of the NSTF. In addition, a separate effects type model was developed to simulate the pressure drop of the RCCS inclusive of the air stack.

fins or ribs could be installed on the inner walls of the air channel to enhance turbulence and heat transfer.

Above the heated zone the flow channel expands to a cross section of 1.32 m (52 in.) x 0.456 m (18 in.) and two flow paths are provided. The main path for the experiments is upward through an "S" curve and then vertically through the building roof. This provides a stack for natural convection nearly 15.2 m (50 ft) in vertical length. The top of the stack is 6.1 m (20 ft) above the roof. The second flow path contains a fan with a variable motor speed and a damper. This feature is provided for forced convection tests, when the system is at very low temperature and a controlled air flow rate is desired. Heat input to the guard vessel is provided by an assembly of electrical heaters that are fastened to a 0.635 cm (0.25 in.) stainless steel plate. Heat is transferred through the plate and then conducted across a small gap to the guard vessel surface. Power to the heaters is computer controlled based on signals from system thermocouples.

The data acquisition system (DAS) was capable of sampling 300 channels, most of which are dedicated to thermocouples located in the heated zone. The DAS stores all its data on disk and selected channels may also be displayed on CTRs and hardcopy. The computer was programmed to use on-line data to compute system parameters for real-time display and hardcopy. The heater power and control system design and the data acquisition system are shown in Fig. 5. In an NSTF facility adapted for RCCS experiments, the DAS system will be completely renovated to satisfy the RCCS needs.

Instrumentation is provided to measure local surface temperatures, local bulk air temperatures, local and bulk air velocities, air volumetric and mass flow rates, the total normal radiative heat flux, and electrical power to the heaters. The instrumentation consists of thermocouples, Pitot-static traversing probes, a Pitot-static air flow "rake," differential pressure transducers, radiation flux transducers, an anemometer and air pressure and humidity gages. Data from these measurements are used to evaluate the heat removal performance for particular configurations and testing conditions. The primary measurement objective was to determine the local and bulk heat flux transport rates and associated heat transfer coefficients. In an NSTF facility adapted for RCCS experiments, the instrumentation will be augmented to satisfy the RCCS needs.

A CFD model was developed to simulate the thermal-hydraulic performance of the NSTF facility. In this model the assumptions were made that each tube behaves as if there was an infinite number of tubes, and the inlet section of the tubes was properly rounded to reduce the inlet pressure loss coefficient to a value of 0.05. The model (Fig. 6) includes the reactor vessel wall, one-half of one tube, one-half of the gap between tubes (assumption of symmetry), a 2.54 carbon steel plate, and a 15.24 insulation plate (hydrous calcium silicate, Johns Manville Thermo-12 insulation). The gap between the tube and the reactor vessel, as well as the gap between the tube and the carbon steel plate is 10.1 cm. In the flow direction, only the heated section was modeled. Pressure drops for the sections of the NSTF flow path that were not directly modeled were accounted as discussed in section 2.3.

Figure 7 shows in scale a cross section of the NSTF flow path and two RCCS tubes inside this flow path. Actually, up to twelve RCCS tubes (tubes plus gap region between tubes) can be placed inside the NSTF flow path to experimentally study the thermal performance of the RCCS. In this arrangement, the heated wall of the facility channel will simulate the wall of the reactor vessel, which is the heat source of the RCCS, and the other channel wall will simulate the insulation of the inner surface (reactor cavity side) of the RCCS downcomer. Measurements will be performed in the central tube, and possibly in some adjacent tubes, while the other tubes will provide the proper radiative surfaces for the simulation of the actual RCCS-tube configuration.

$$\int_0^{H_h} (\rho_o - \rho) g dh + g H_s (\rho_o - \rho_s) = \rho_o g \left\{ \left[1 - \frac{\ln(T_e/T_o)}{T_e/T_o - 1} \right] H_h + \left(1 - \frac{\rho_s}{\rho_o} \right) H_s \right\} \tag{5}$$

$$\Delta\rho_f = \frac{2 f_h W^2}{D_h \rho_0 T_0 A_h^2} \int_0^{H_h} \left(T_0 + \frac{T_e - T_0}{H_h} h \right) dh = \frac{f_h W^2}{D_h \rho_0 A_h^2} \left[H_h \left(1 + \frac{T_e}{T_0} \right) \right] \tag{6}$$

where

W	=	air mass flow rate
D_h	=	hydraulic diameter of the heated section
A_h	=	flow area at heated section
f_s	=	friction factor
ρ	=	air density
ρ_o	=	air density at the inlet of the heated section
ρ_s	=	air density at the exit of the heated section
T_o	=	air temperature at the inlet of the heated section
T_e	=	air temperature at the exit of the heated section

The acceleration pressure drop is

$$\Delta p_a = \frac{W^2}{A_h^2} \left(\frac{1}{\rho_s} - \frac{1}{\rho_0} \right) \tag{7}$$

The friction coefficient f_h can be computed from

$$f_h = 0.0791 \mathrm{Re}_h^{-0.25} \tag{8}$$

For a rectangular duct Petukhov [3] gives the correlation

$$f_h = 0.25 \left[1.82 \log(\mathrm{Re}/8) \right]^{-2} \tag{9}$$

For the RCCS duct the friction factor values given by Eqs (8) and (9) differ by 1.7 %. Thus, either of them can be used. A small computer program was written that computes Δp_{other} from Eqs (4), (5), (6), (7) and (8).

The pressure drop Δp_{other} can be approximated by

$$\Delta p_{other} = K_L \frac{W^2}{2 \rho_0 A_h^2} \tag{10}$$

core block-heights, under the constraint that the peak fuel temperature does not exceed 1600 °C. Similar scoping analyses by GA (Ref. 5) report peak vessel temperatures that do not exceed 533 °C. These peak vessel temperatures are not drastically higher than those of the GT-MHR.

In October 2004, INEEL provided to ANL plant information for an NGNP design having also a core outlet temperature of 1000 C. For this design RELAP HPCC and LPCC transient analyses were performed by ANL. The LPCC transient gave a higher peak fuel temperature, which is reached at 76.7 hr from transient initiation. RELAP predicted at 76.7 hr an outside reactor vessel peak temperature of 467 °C at 6 m from the bottom of the lower reflector and an RCCS flow rate of 13.32 kg/s.

CFD RCCS simulations were performed:

(a) For a uniform reactor vessel temperature of 480 °C, and an RCCS flow rate of 14.3 kg/s (GT- MHR steady state).
(b) For a uniform reactor vessel temperature of 560 °C.
(c) For a peak reactor vessel temperature of 560 °C
(d) For the reactor vessel temperature distribution and RCCS flow rate at 76.7 hr determined by the ANL RELAP analysis of the LPCC transient mentioned above.

3.1 Uniform Reactor Vessel Temperature of 480 °C (GT-MHR Steady State)

In this simulation the following boundary conditions were used: a temperature of 480 °C for the outer reactor vessel surface; a temperature of 43 °C at the outer surface of the insulation; a tube flow rate as provided in Ref. 1; and an air inlet temperature of 43 °C (Ref. 1).

Figure 8 shows the temperature distribution on a tube cross-section at 14.9 m from the tube inlet (tube outlet at 15.6 m). This distribution is very asymmetric and reaches a minimum around the center of the back half of the tube. The maximum to minimum difference is 137 °C. The temperature distribution on the front and back walls of the tube are nearly uniform, but there is a large temperature variation from front to back on the side wall of the tube. This variation is about 111 °C.

Figure 9 shows the heat transfer coefficient along the axis of the front, side and back tube walls as predicted by the high-Re number model of turbulence. These heat transfer coefficients are based on the fluid temperature of the cells next to the wall. As it will be shown later these coefficients are more meaningful than coefficients based on the bulk air temperature. Figure 10) shows the variation of the heat transfer coefficient around the tube at 14.9 m from the tube inlet. These figures show a variation of the heat transfer coefficient around the tube as well as along the tube. The heat transfer coefficient is significantly higher on the side wall, and at any cross-section of this wall the variation of the heat transfer coefficient from the front to the back end of this wall is significantly higher than in the other two tube walls (front and back).

Figure 11 shows the variation of the heat flux around a tube at heights of 1.0m, 7.8 m, and 14.9 m. At 1.0m the heat flux peaks on the front wall, then at higher locations the peak moves to the side-wall, and moves from the front section towards the back section of this wall as we move higher from the bottom to the top of the tube.

zone where there is a large temperature variation along the long axis of the tube (from front to back). It is seen from this figure that the velocity variation is mainly due to the density variation with temperature, which varies significantly as we move from the front face to the back face of the tube.

In the GT-MHR design of GA, the distance between the outer surface of the reactor vessel and the front side of the RCCS tubes is 0.77 m, and the distance between the downcomer insulation and the back side of the RCCS tubes is 0.38m (GT-MHR cavity). In the NSTF facility these distances would be of the order of 0.1 m (NSTF cavity). This has an effect on the view factors between the reactor vessel and the RCCS tubes. To asses this effect on the RCSS performance parameters, simulations were performed for a reactor vessel temperature of 480 °C and a distance of 0.1 m between the reactor vessel and the front tube wall, as well as between the downcomer insulation and the back tube wall.

For the NSTF cavity, the power removed by the RCCS increased by 11%. Figures 18 and 19 show the heat transfer coefficient along the axis of the front and side RCCS walls for the "GT-MHR" and the "NSTF" cavity. These coefficients are based on the bulk air temperature. The "NSTF" cavity gives a higher heat transfer coefficient, but the difference is small. Also these Figures show sharp variations of the heat transfer coefficient near the tube inlet and outlet. Figure 20 shows the variation of the air temperature and of the tube temperature from tube-front to tube-back at a cross-section at 14.9 m from the tube inlet. The temperature variation is highly asymmetric. At this cross section the air bulk temperature is 273 °C. This temperature is higher than the air temperature next to the side wall along the back-half of this wall. It is clear that because of the highly asymmetric air temperature distribution in the tube, the use of the bulk air-temperature to compute a heat transfer coefficient is not meaningful. Instead, the heat transfer coefficient based on the air temperature in the cells next to the wall is more meaningful. This heat transfer coefficient for the front, side and back wall of the tube is shown in Figs. 21, 22 and 23. The difference, in terms of the heat transfer coefficient, between the "GT-MHR" cavity and the "NSTF" cavity is very small.

The buoyancy driven flow in the reactor cavity does not converge to a steady state (laminar as well as turbulent simulation with the steady state simulator), because the flow may be chaotic. The following figures show air velocity distributions in the "NSTF" cavity assuming laminar flow in the cavity. The simulation with the high Re number k-ε model gives similar results. As Figure 24 shows (a vertical cross section of the cavity through a tube), the flow moves down in the space between the downcomer insulation and the tubes and upwards in the space between the reactor vessel and the tubes. Figure 25 shows velocity contours for the whole cavity assuming laminar flow, and Figure 26 shows the same information as predicted by the high-Re number k-ε model. The maximum velocity is about 1m/sec. Figure 27 shows the velocity distribution in a vertical cross section of the cavity in the gap between two tubes. It clearly shows a complicated flow pattern that may be generated by a chaotic flow. To ascertain that the flow is chaotic a transient simulation is needed.

3.2 RCCS Performance at VHTR Conditions

Uniform Reactor Vessel Temperature of 560° C

For a reactor vessel temperature of 560 °C, the buoyancy force driving the RCCS flow established an air flow rate of 5.223 e-02 kg/sec per RCCS tube. This corresponds to a Re number of 20,030, versus a Re number of 18,780 for the RCCS of the GT-MHR design. The RCCS (292 tubes) removed 5.02 MW versus 3.3 MW removed by the RCCS of the GT-MHR.

VHTR design, was analyzed with STAR-CD at 76.7 hrs using the flow rate and the outer reactor vessel temperature distribution predicted by RELAP (Fig. 37). This distribution has a peak value of 467 °C at 6 m from the bottom of the lower reflector (floor of reactor cavity), and drops significantly below and above this location.

The temperature distribution of the front (hottest) tube wall reaches a peak value of 552.5 K (279.5 °C) at 6.8 m. Figure 38 shows the air temperature distribution along the RCCS tube, and Figure 39 shows the air and tube temperature distribution on a tube cross section at a height of 5.3 m (around the area of the peak wall temperature). The wall temperature around the tube varies by about 111 °C, while the air temperature varies by about 122 °C. Figure 40 shows the variation of the heat transfer coefficient along the axis of the front, side, and back tube walls. This variation is covered well by the variation of the same variables at NSTF (section 4.0). Figures 41, 42, and 43, show the variation of the Nusselt number, Grashof and Rayleigh number, and of the buoyancy number. Their variation is also well covered by the variation of the same parameters at NSTF (section 4.0). Notable is the sharp drop of the Grashof, Rayleigh, and buoyancy numbers after a height of about 8 m (reactor vessel temperature peaks at 6 m).

4.0 NSTF PERFORMANCE

In the effort to demonstrate that all significant fluid flow and heat transfer phenomena in the RCCS, and the range of variation of the parameters describing these phenomena can be simulated at NSTF, NSTF simulations were performed for: (a) a uniform heated wall temperature of 480 °C, and (b) for a uniform heated wall temperature of 677 °C

4.1 Uniform Heated Wall Temperature of 480 °C

For this simulation, the air velocity at the tube inlet was set to 4.353 m/s, based on a GT-MHR RCCS flow rate of 14.3 kg/s at steady state conditions. For a uniform heated wall temperature of 480 °C, it was computed (from the pressure drop model of section 2.3) that the pressure losses at NSTF can accommodate a larger flow rate than that corresponding to an air velocity of 4.353 m/s. Thus, the velocity of 4.353 m/s can be achieved at NSTF by properly adjusting the pressure drop damper. At the outer surface of the insulation a constant temperature of 43 °C was used as a boundary condition. The air inlet temperature was also set to 43 °C (GA RCCS air inlet temperature).

This simulation predicted an air outlet temperature (bulk) of 181.5 °C, a reactor vessel heat flux of 10.14 kw/m2, and a heat removal rate of 6.9 kw/tube. Figure 44 shows the air and tube-wall temperature distribution at the top of the heated section (6.7m). The tube temperature varies from 620 K (front) to 514 K (back), while the air temperature varies from 411 K to 579 K. These temperatures variations are similar to those near the outlet of the RCCS tubes for the same reactor vessel temperature. Figure 45 shows the variation of the heat transfer coefficient along the axis of the front, side and back tube walls. This variation is also similar to that in the RCCS. Figures 46 and 47 show the variation of the heat transfer coefficient and of the heat flux around the tube. Figure 48, shows the variation of the heat transfer coefficient assuming a constant air thermal conductivity. Figures 45 and 48 show that the increase in the heat transfer coefficient with tube height is due to the increase in the thermal conductivity of air as its temperature increases.

Figure 49 shows the variation of the Reynolds (Re) number along the tube height. For a reactor vessel temperature of 480 °C, the variation of the Re number in the plant RCCS tube and the NSTF tube is nearly identical. However, because the plant RCCS tube is longer, in plant RCCS

As Figure 49 shows, in the plant RCCS as the air is heated up in the tubes its viscosity increases and the Re number drops at the top of the tube at a value of 12000. Such low Re number values can also be simulated in the NSTF (shorter tube) by increasing the flow pressure losses and reducing the flow rate. For example, as Figure 49 shows, for a heated wall temperature of 677 °C and an air inlet flow rate of 4.52 m/s the Re number along the NSTF tube varies from 17300 to 11900 which covers well the range of Re number variation in the RCCS.

5.0 CONCLUSIONS

In the RCCS, strong 3-D effects result in large heat flux, temperature, and heat transfer variations around the tube wall. Higher temperatures in the front tube wall and air density variations with temperature lead to significant buoyancy inside the tube which reduces turbulence, thermal mixing, and the overall heat transfer coefficient. The increase in air thermal conductivity with temperature results in an increase of the heat transfer coefficient with tube height. The increase of viscosity with temperature leads to a significant decrease of the Reynolds number with tube height. Radiation between the RCCS tube walls redistributes the heat flux. There is a large difference in the heat transfer coefficient predicted by turbulence models and heat transfer correlations, and this underscores the need of experimental work to validate the thermal performance of the RCCS. Simulations of the RCCS at the NSTF facility can cover all important fluid flow and heat transfer phenomena, and the whole range of variation of the important thermal-hydraulic parameters in the RCCS.

Reference:

1.0 Gas Turbine-Modular Helium Reactor (GT-MHR) Conceptual Design Description Report, Revision 1, GA Project No 7658,General Atomics, San Diego,CA (1996). (nov)

2.0 C. P. Tzanos, "Passive Decay Heat Removal in the Reactor Cavity Cooling System," Trans. Am. Nucl. Soc., November 2004.

3.0 B. S. Petukhov and A. F. Polyakov, Heat transfer in Turbulent Mixed Convection, Hemisphere Publishing Company,1988 (nov)

4.0 P. D. Bayless, "VHTR Thermal-Hydraulic Scoping Analyses Using RELAP5-3D/ATHENA", Global 200, pp 312-319, New Orleans, LA, November 16-20,2003.

5.0 NGNP Point Design - Results of the Initial Neutronics and Thermal-Hydraulic Assessments During FY-03. INEEL/EXT-03-00870 Rev.1. (oct wei)

6.0 J. D. Jackson, M. A. Cotton and B. P. Axcell, "Studies of Mixed Convection in Vertical Tubes," Int. J. Heat and Fluid Flow, 10, pp 2-15 (1989)

7.0 Heat Transport and Afterheat Removal for Gas Cooled Reactors Under Accident Conditions, IAEA-TECDOC-1163, IAEA-Vienna, 2000 (jan)

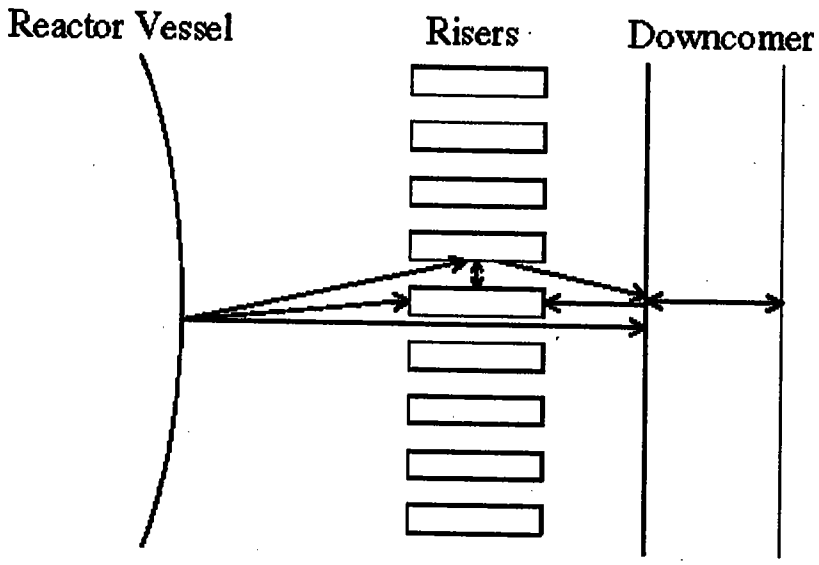

Figure 1. Horizontal cross-section of the GT-MHR RCCS

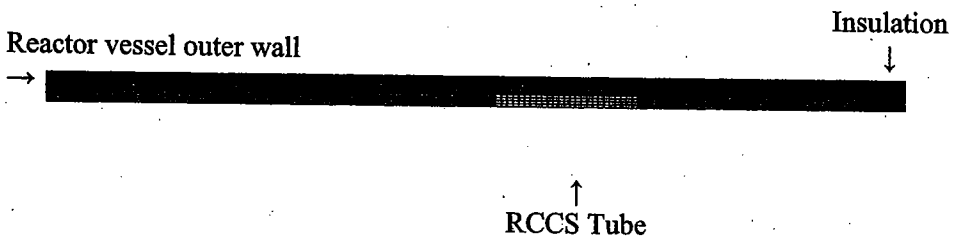

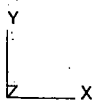

Figure 2. Cross-section of simulated RCCS configuration (plant geometry)

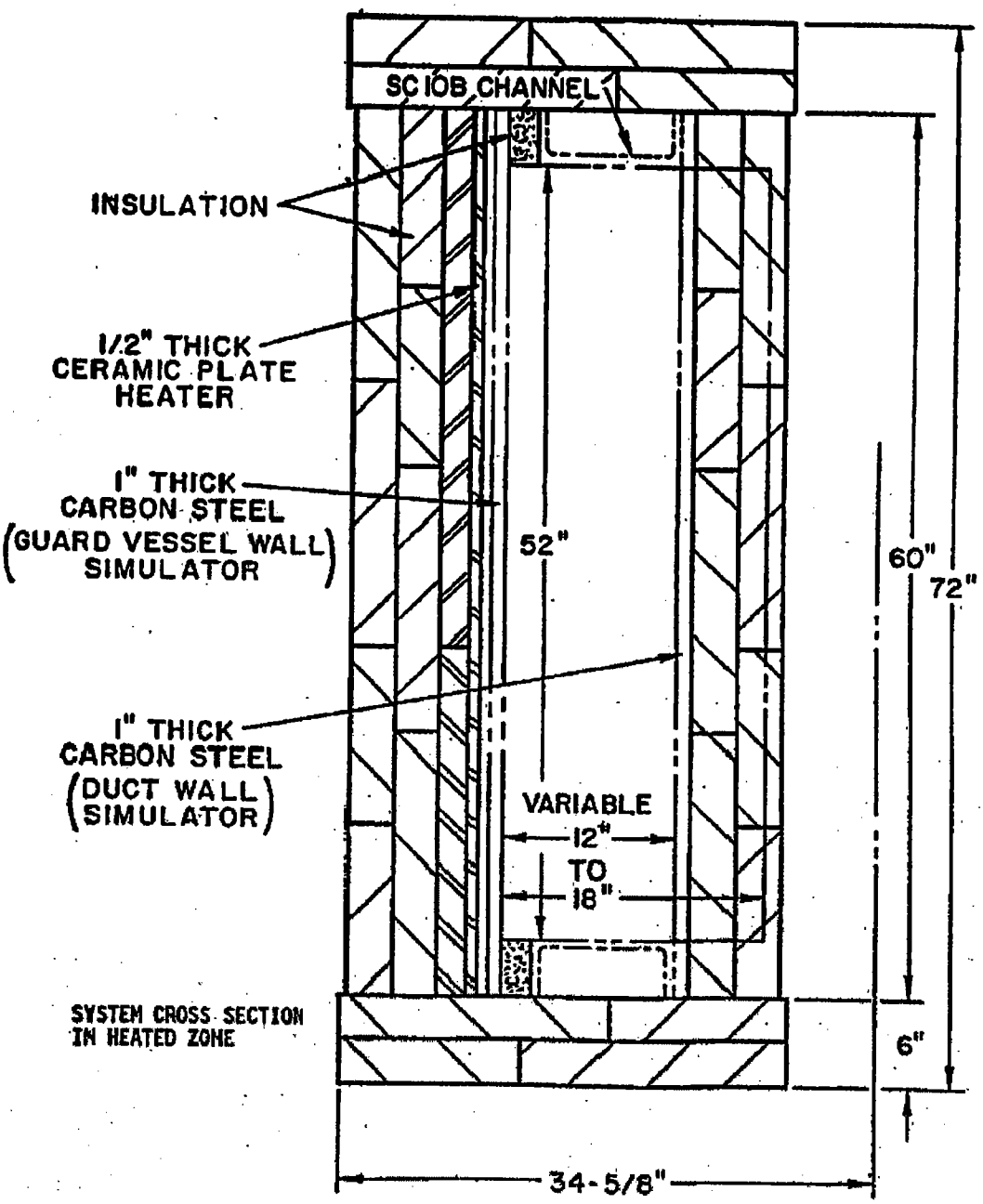

Figure 4. NSTF test section

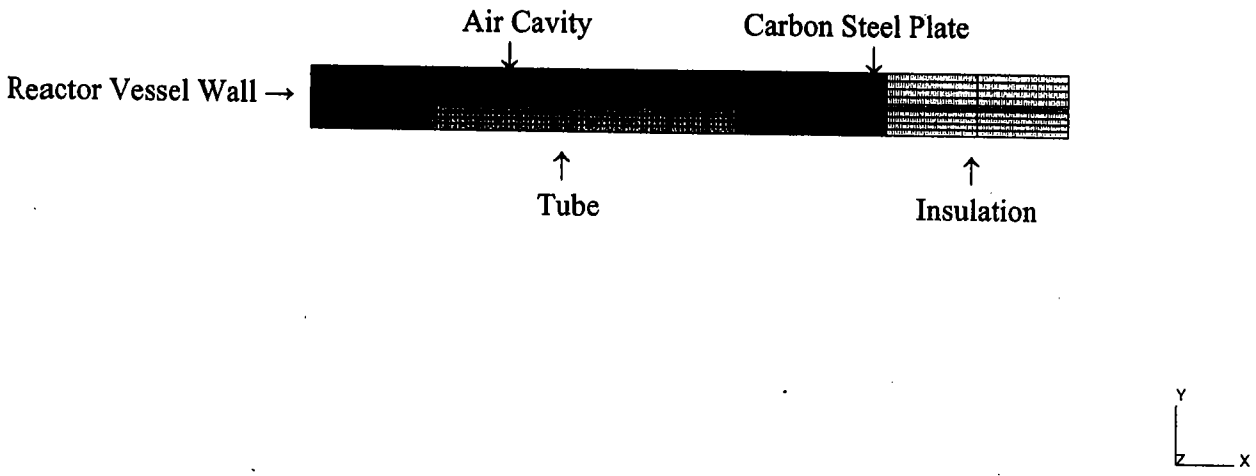

Figure 6. Cross-section of RCCS model at NSTF

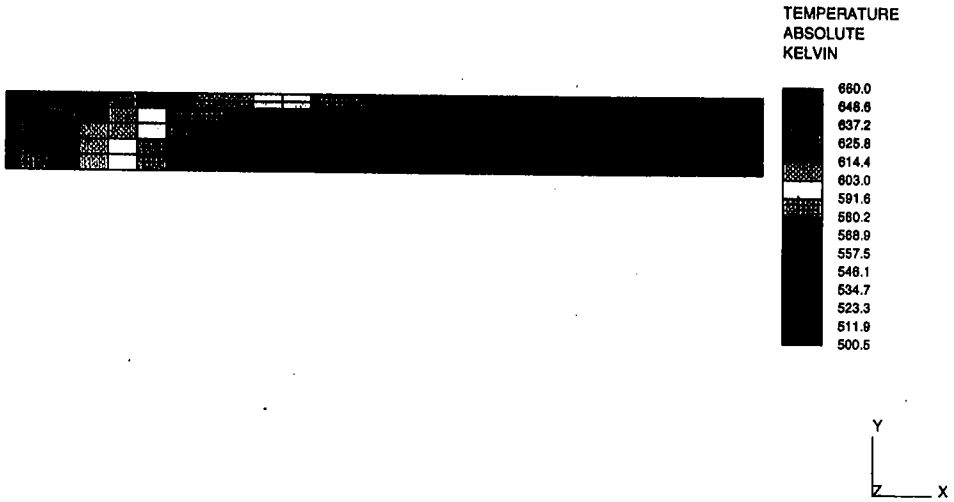

Figure 8. Tube temperature distribution at 14.9 m, reactor vessel temperature of 480 °C

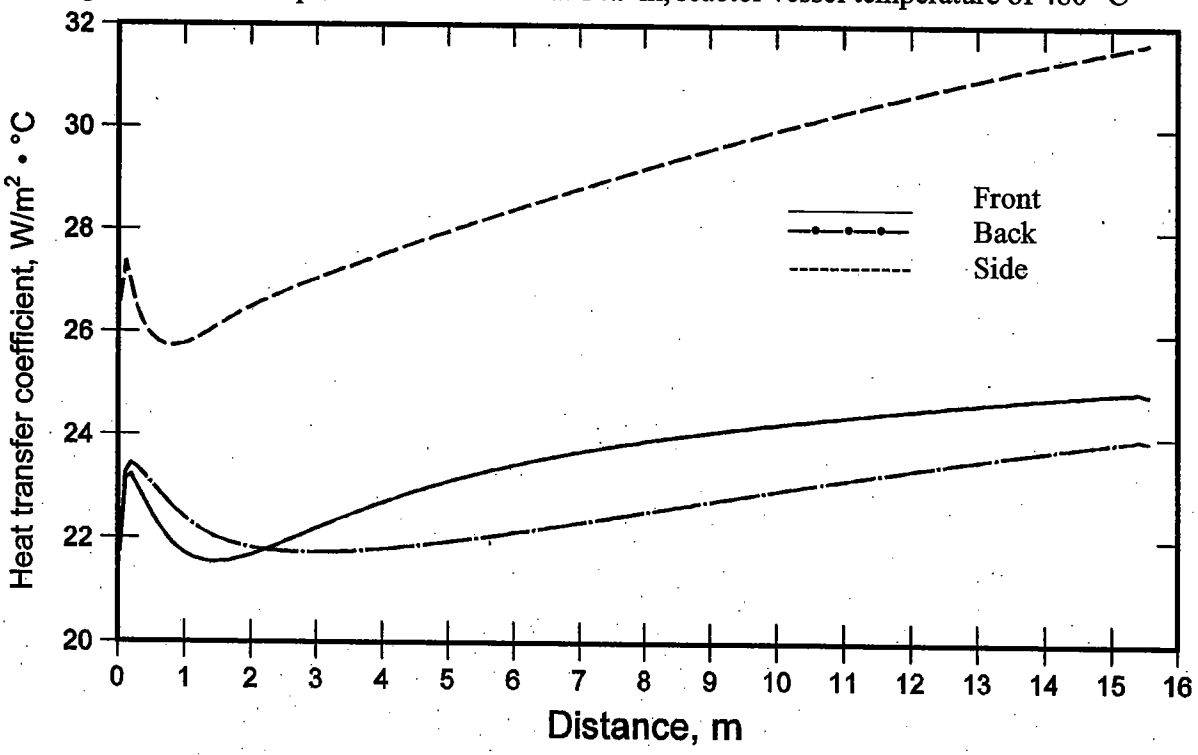

Figure 9. Heat transfer coefficient for reactor vessel temperature 480°C.

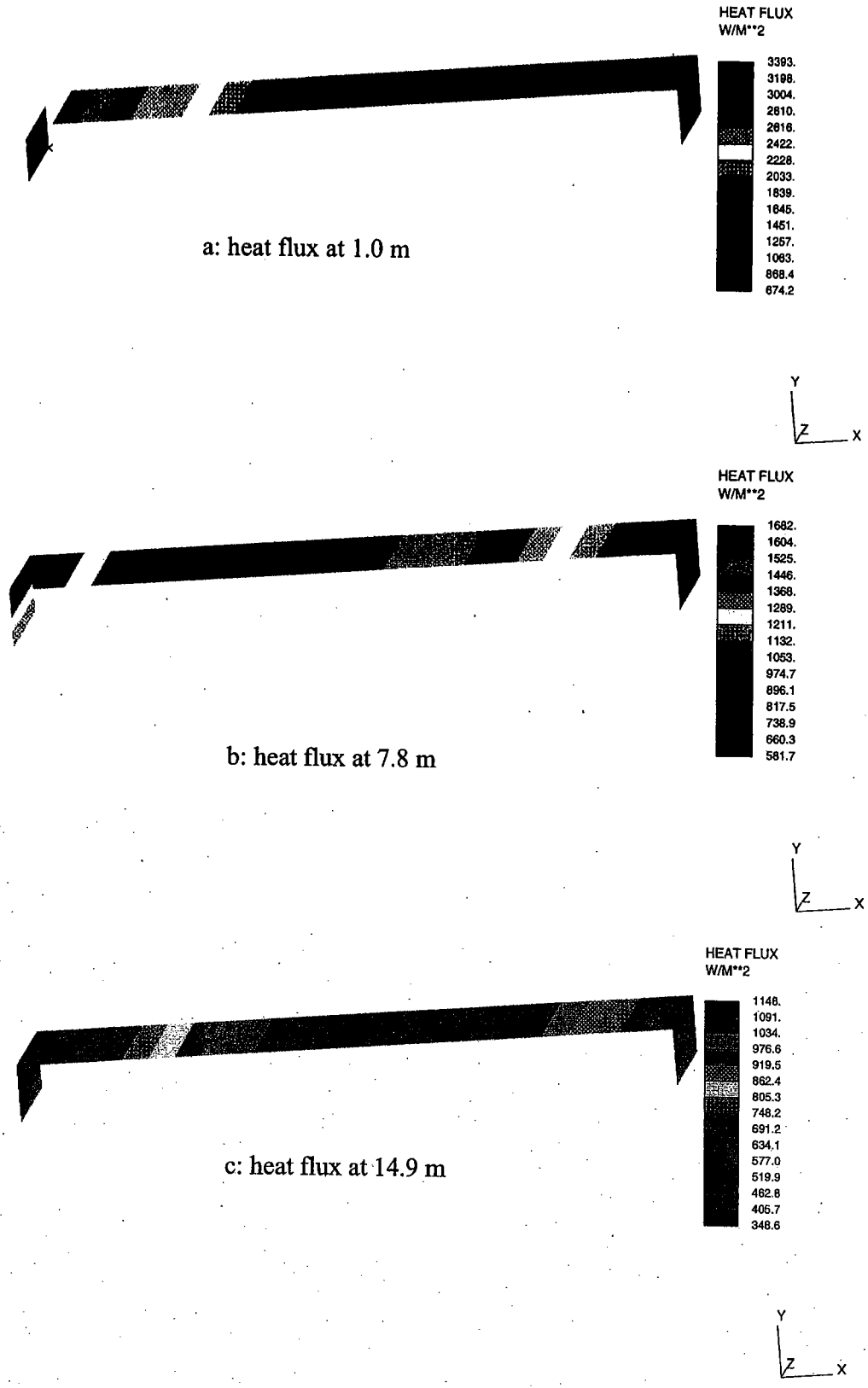

a: heat flux at 1.0 m

b: heat flux at 7.8 m

c: heat flux at 14.9 m

Figure 11. Heat flux distribution, reactor vessel temperature of 480 °C.

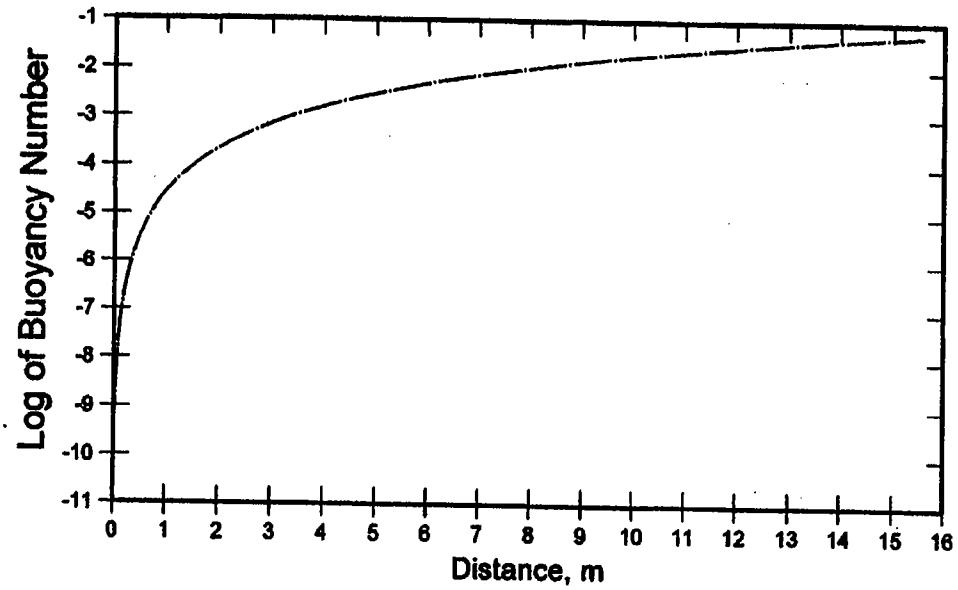

Figure 14. Buoyancy Number, reactor vessel temperature of 480 °C

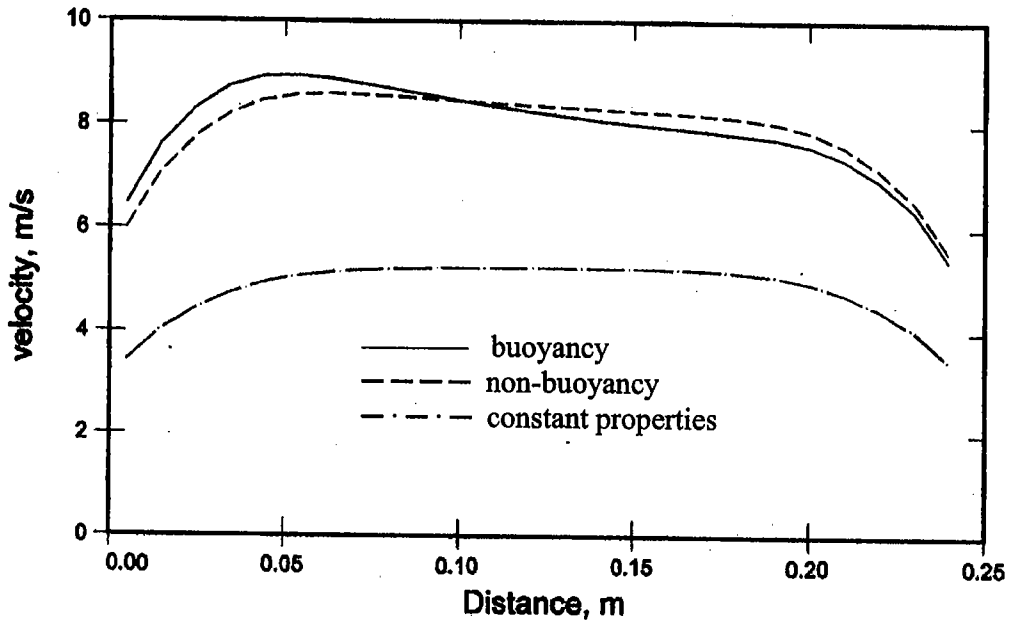

Figure 17. Velocity distribution at 12.35 m for reactor vessel temperature of 480 °C

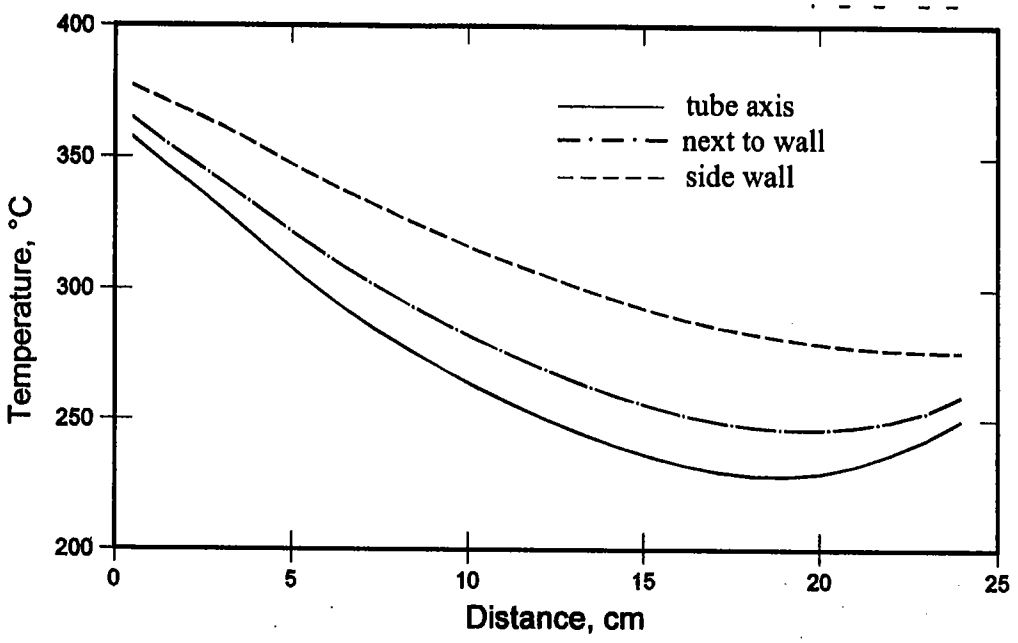

Figure 20. Air and tube wall temperature variation at 14.9 m (GT-MHR cavity)

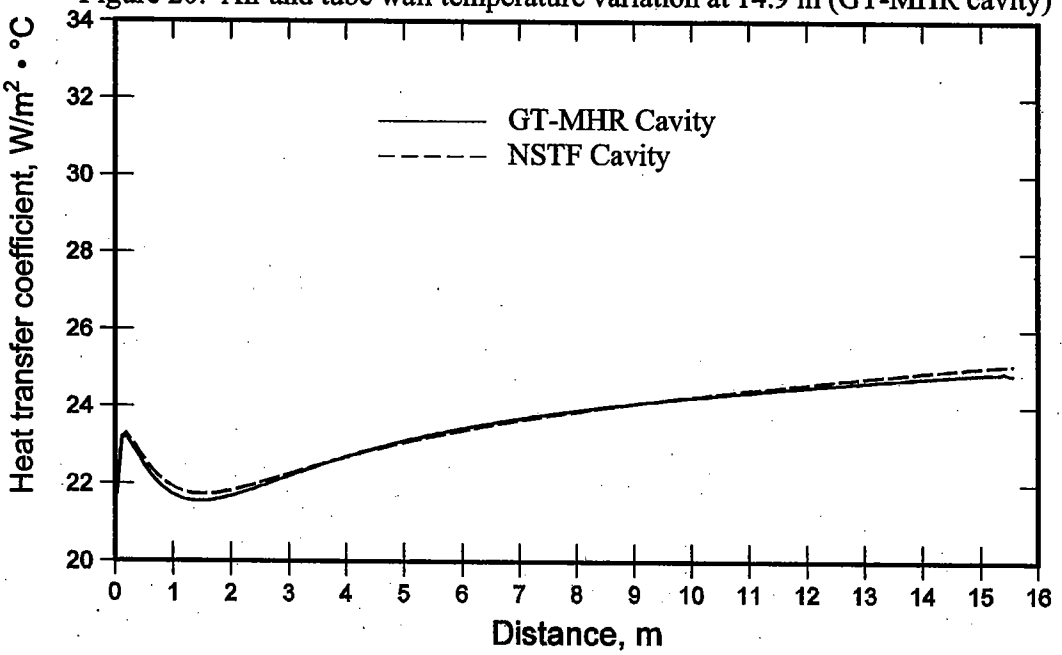

Figure 21.Cavity parametrics: heat transfer coefficient along the axis of the front wall

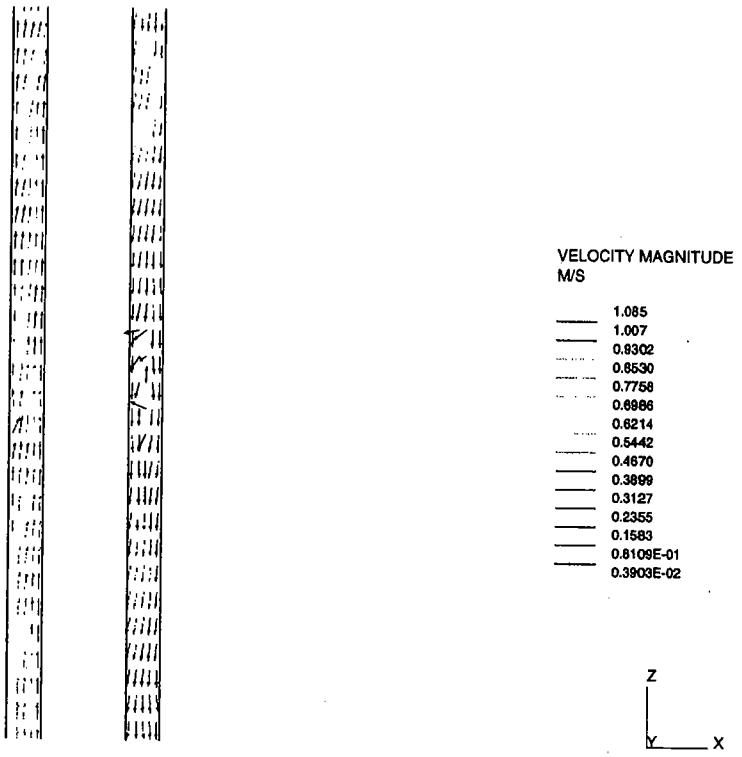

Figure 24. Air-flow in the "NSTF" cavity

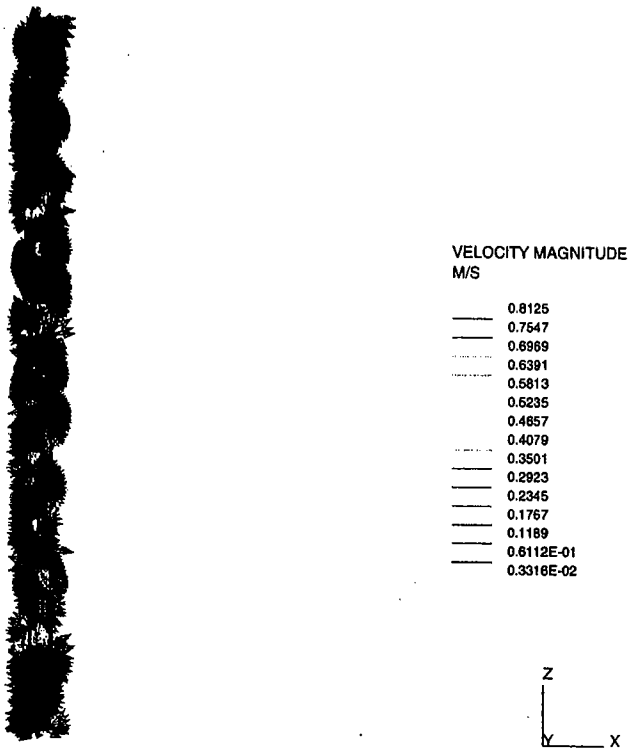

Figure 27. Velocity distribution in the gap between tubes

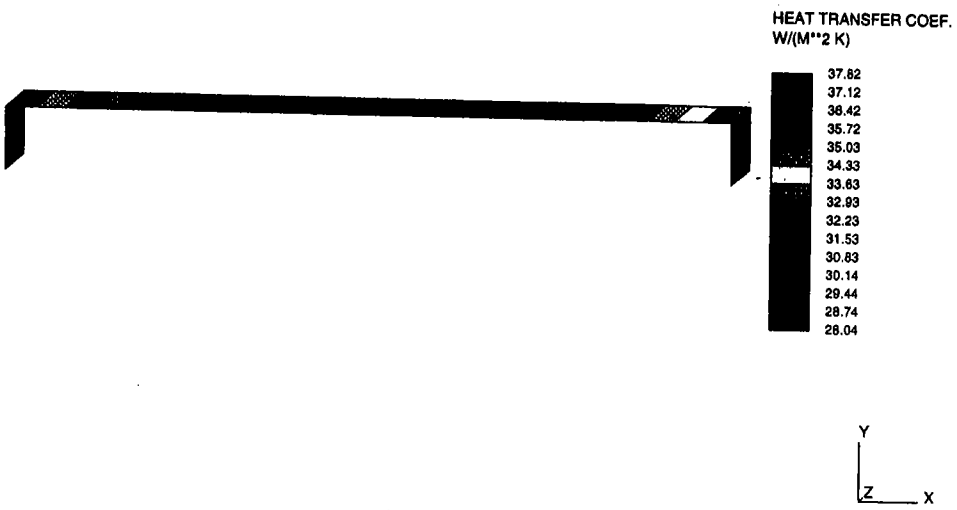

Figure 30. Heat transfer coefficient around the tube at 14.9 m (uniform reactor vessel temperature of 560 °C)

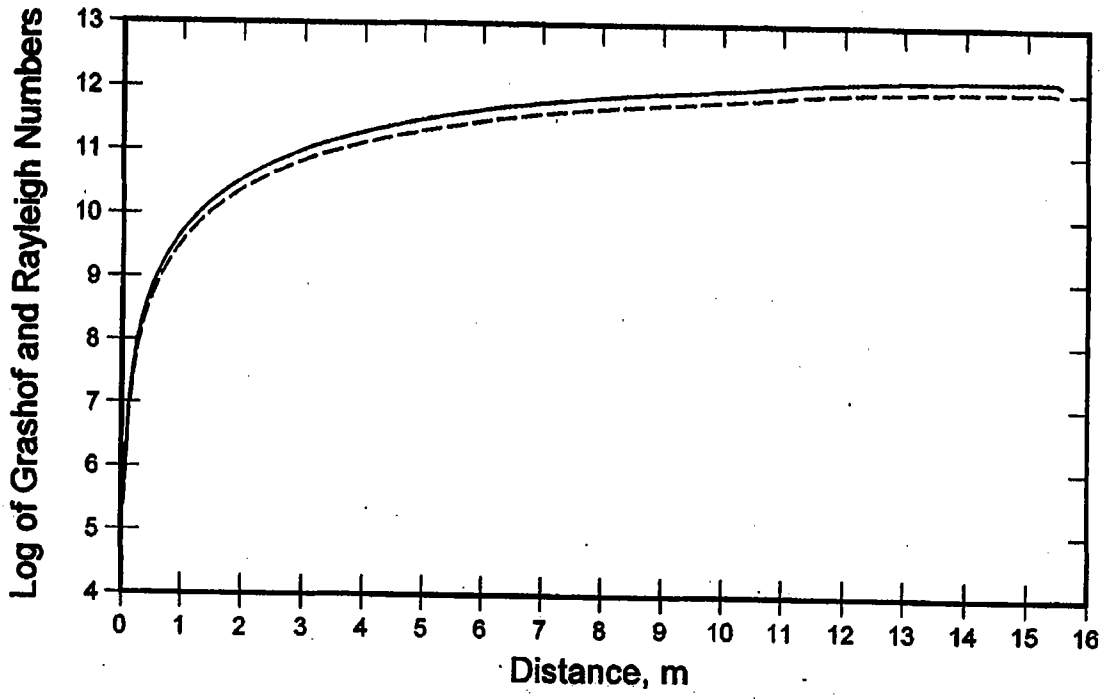

Figure 33. Grashof and Rayleigh numbers along the axis of the front tube wall (non-uniform reactor vessel temperature - peak of 560 °C).

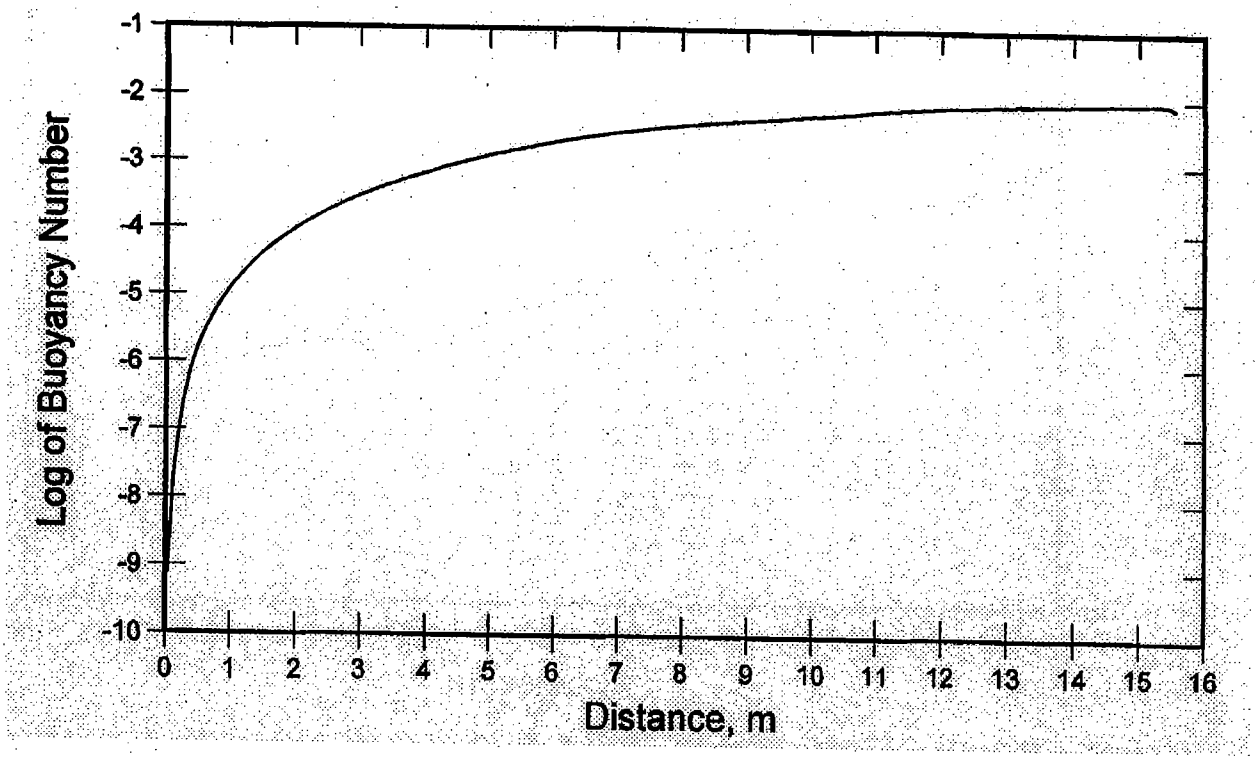

Figure 34. Buoyancy number along the axis of the front tube wall (non-uniform reactor vessel temperature - peak of 560 °C).

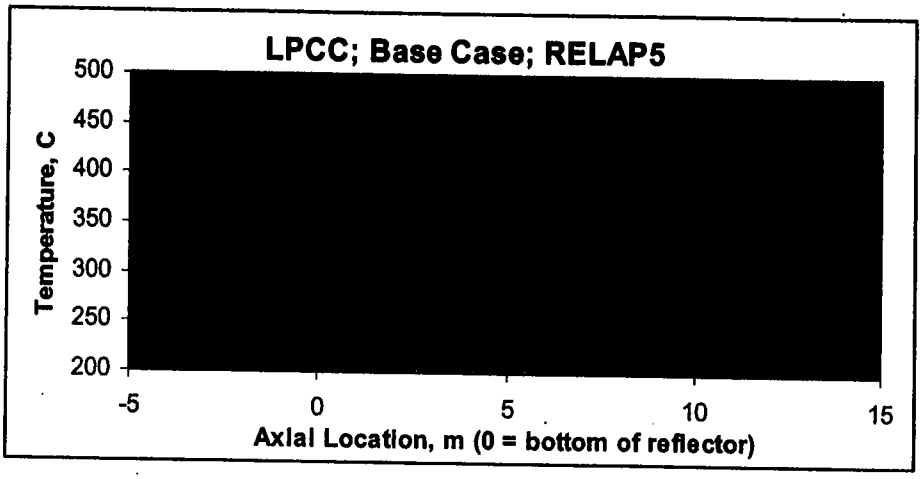

Figure 37. Reactor vessel temperature distribution (VHTR1000)

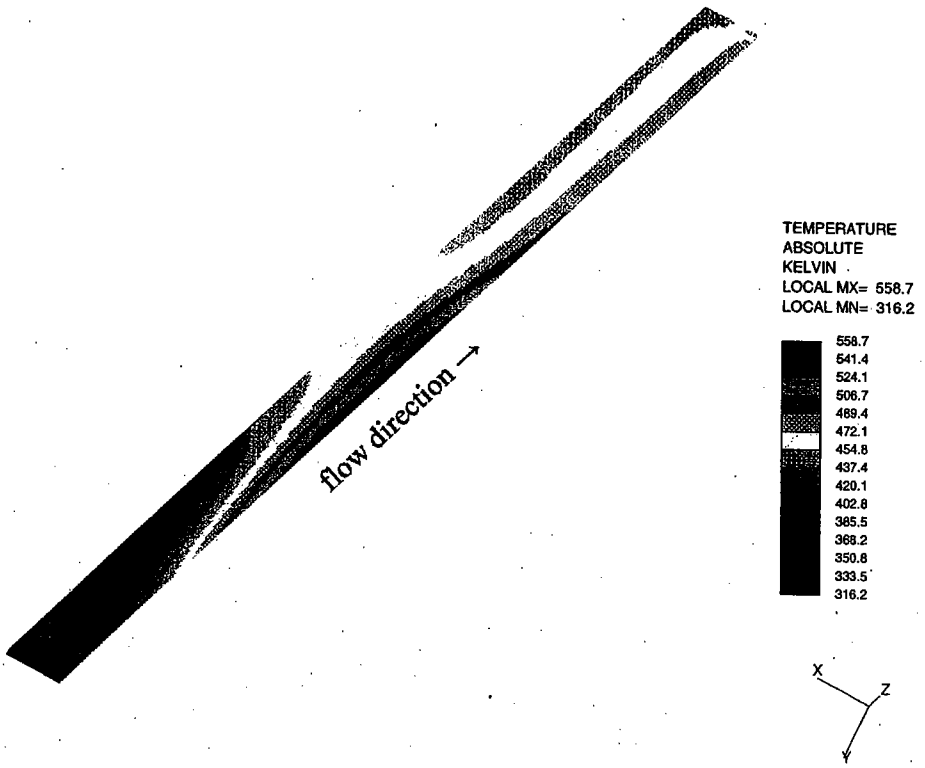

Figure 38. Air temperature distribution along the RCCS tube (VHTR1000)

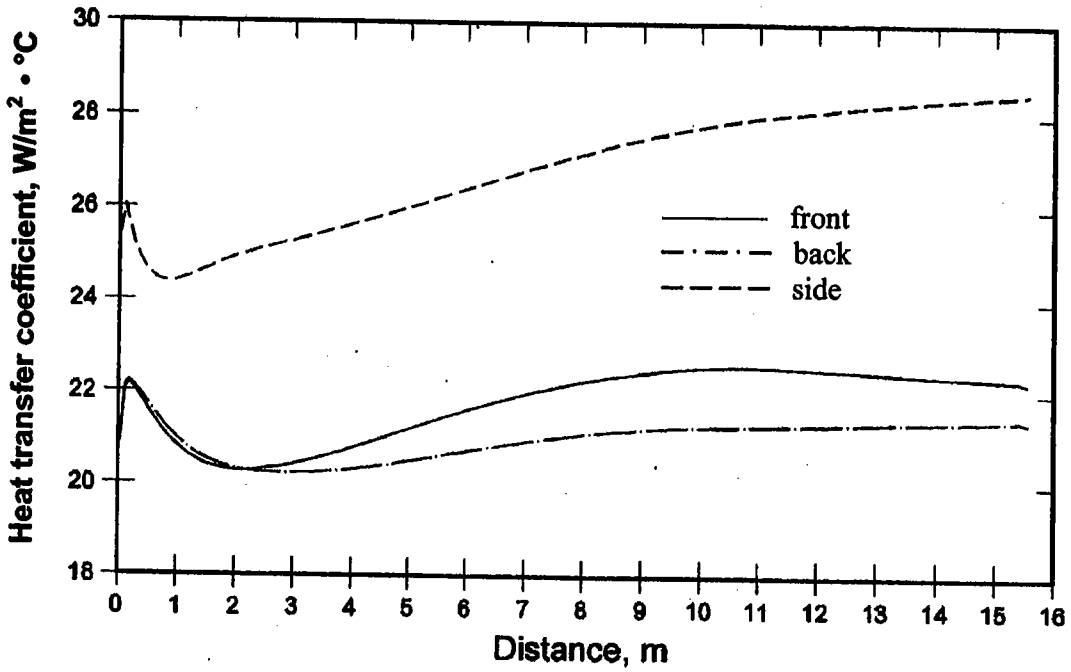

Figure 40. Heat transfer coefficients (VHTR1000)

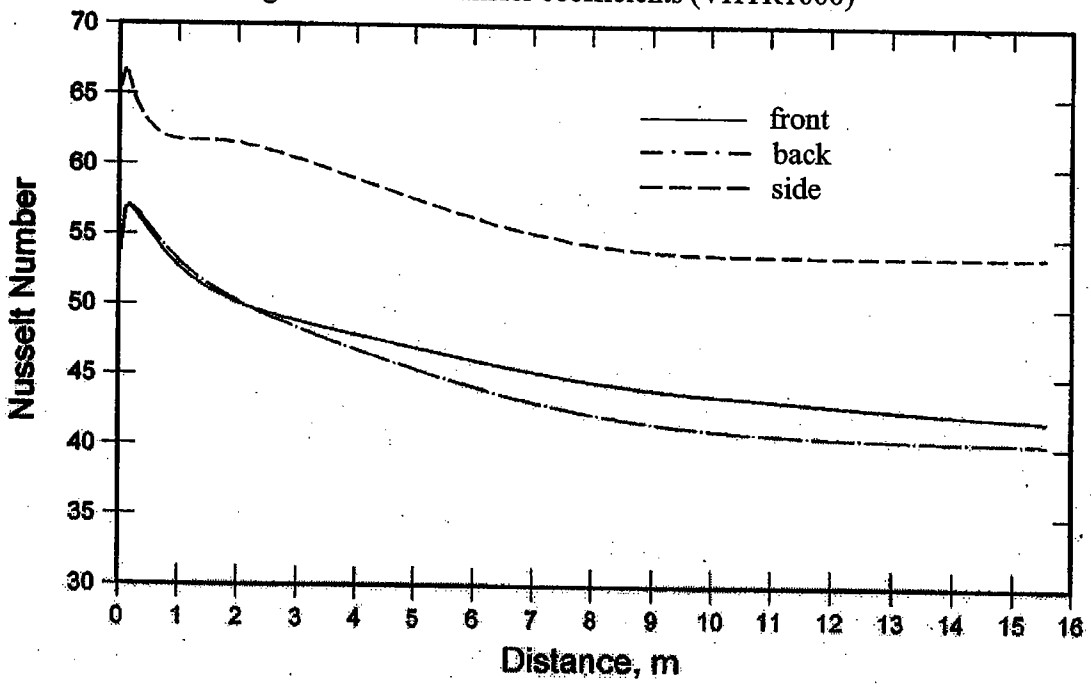

Figure 41. Nusselt number vs. tube height (VHTR1000)

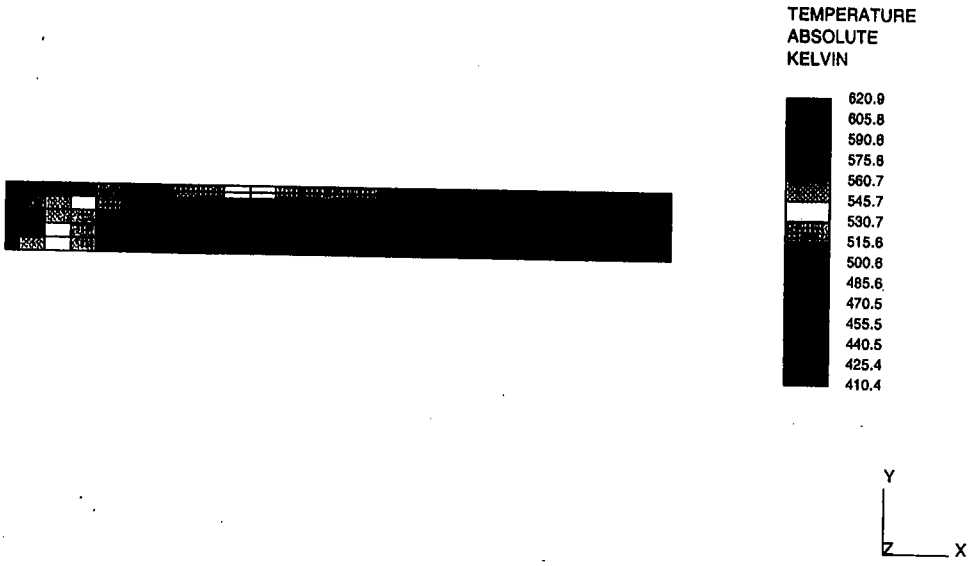

Figure 44. NSTF tube temperature distribution at 6.7 m (heated wall temperature of 480 °C).

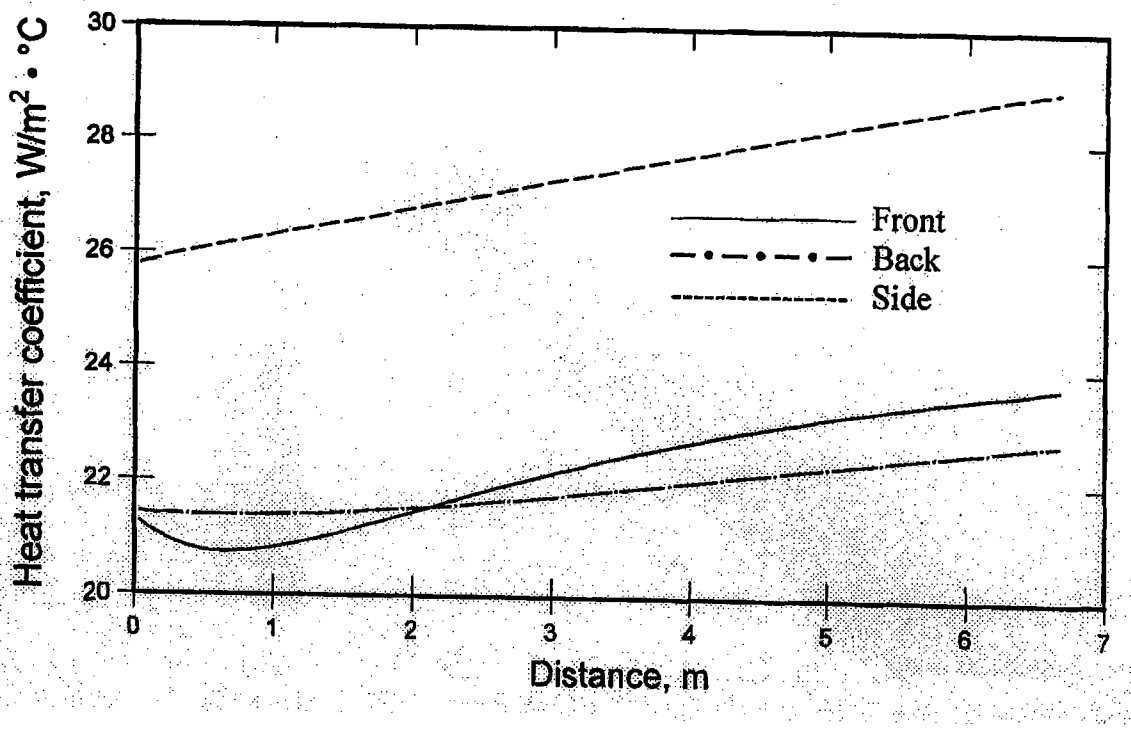

Figure 45. NSTF heat transfer coefficient (heated wall temperature of 480 °C)

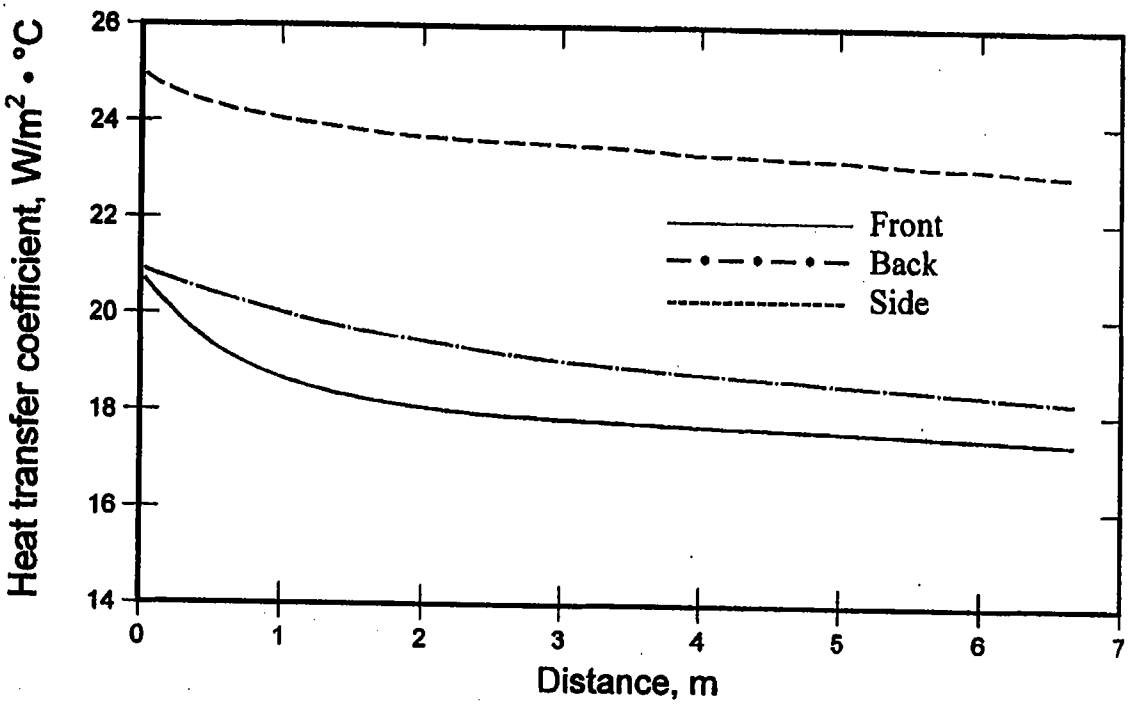

Figure 48. Heat transfer coefficient for a constant air thermal conductivity (NSTF heated wall temperature of 480 °C).

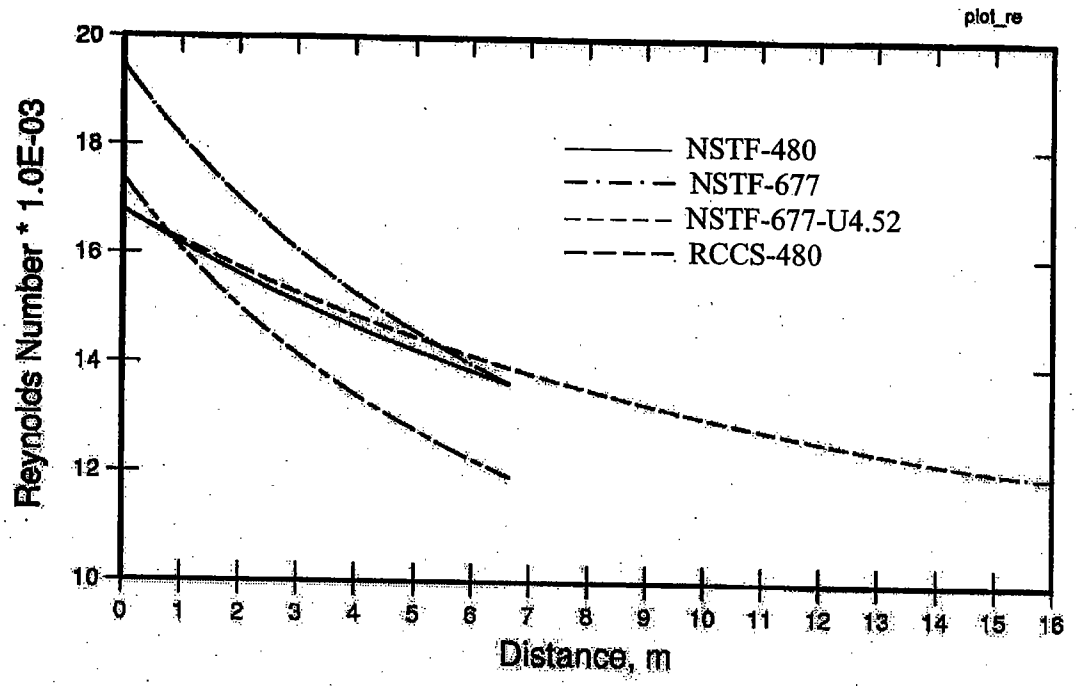

Figure 49. Reynolds number versus tube height.

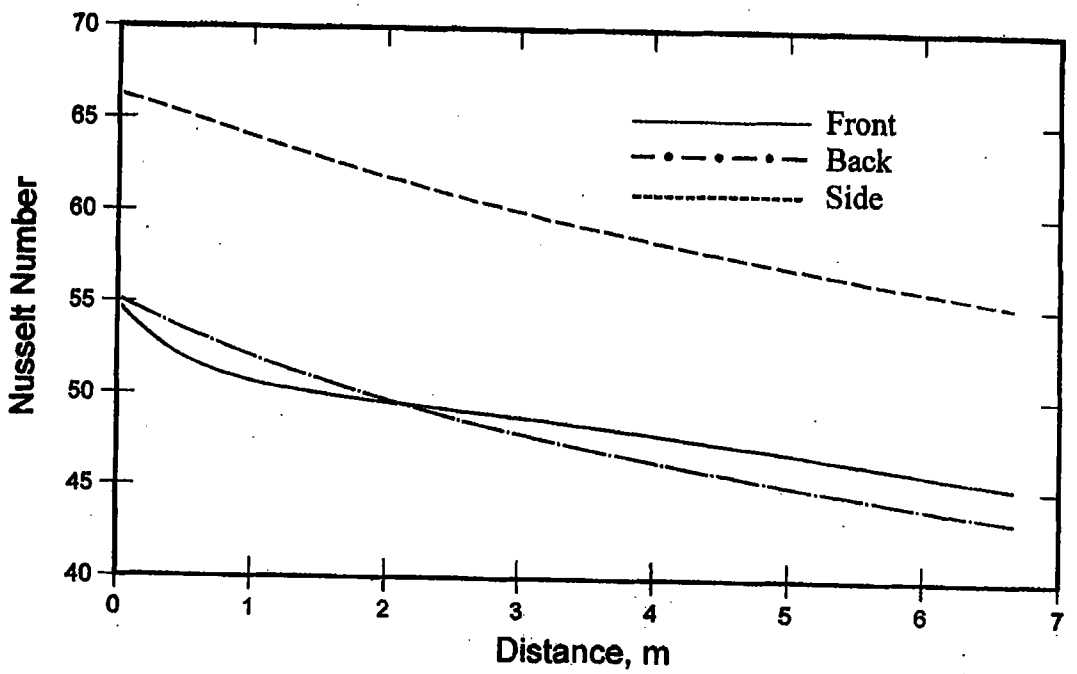

Figure 52. Nusselt number versus NSTF tube height (NSTF heated wall temperature of 480 °C).

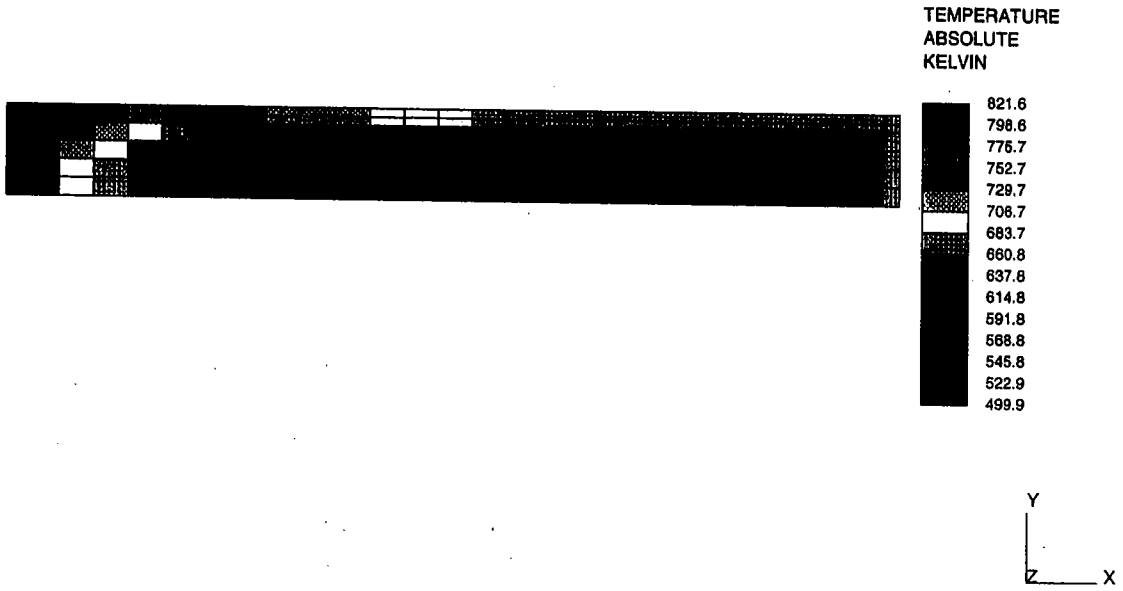

Figure 55. NSTF tube temperature distribution at 6.7 m (heated wall temperature of 677 °C).

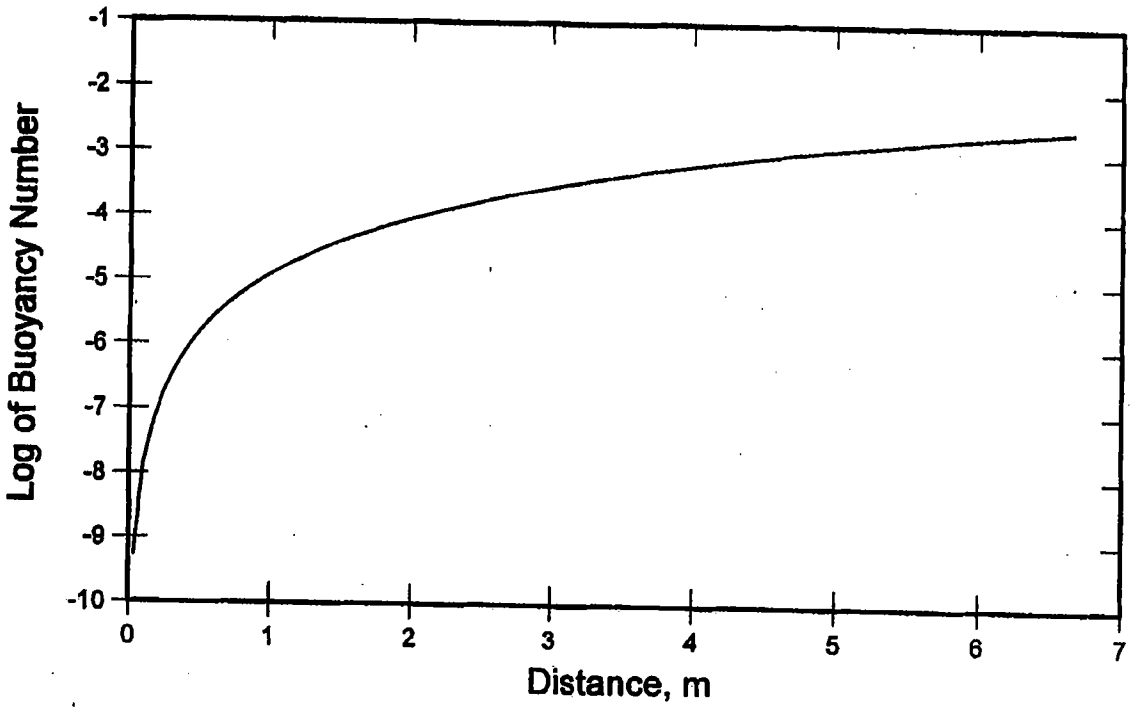

Figure 58. Buoyancy number (NSTF heated wall temperature of 677 °C).

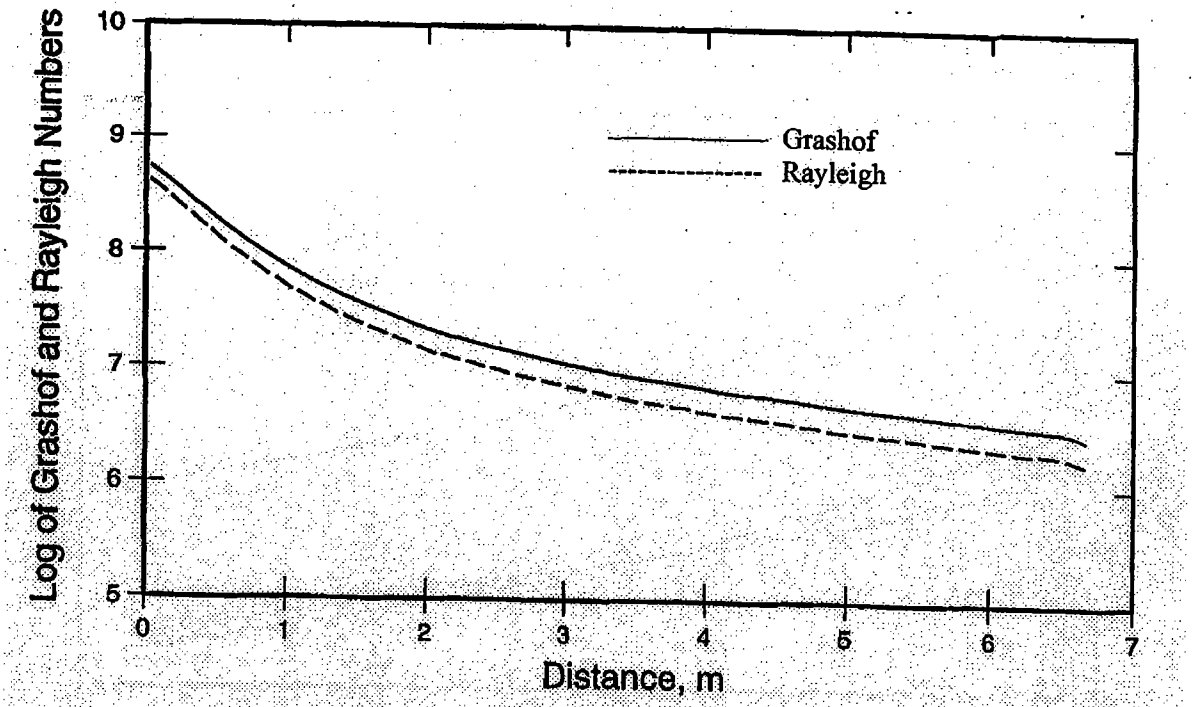

Figure 59. Grashof and Rayleigh numbers; front wall of NSTF tube (based on hydraulic diameter and heated wall temperature of 677 °C).

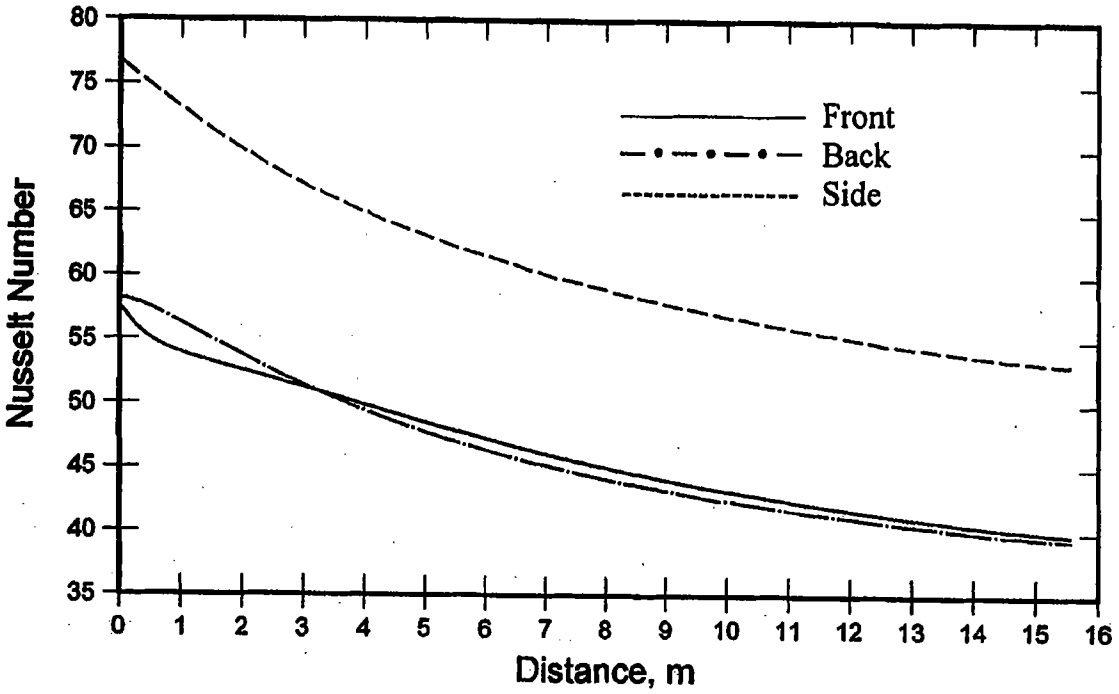

Figure 62. Nusselt number along the axis of the RCCS tube walls (reactor vessel temperature of 560 °C).

Nuclear Engineering Division
Argonne National Laboratory
9700 South Cass Avenue, Bldg. 208
Argonne, IL 60439-4842

www.anl.gov

UChicago ▶ Argonne LLC

A U.S. Department of Energy laboratory managed by UChicago Argonne, LLC